Biochimica et Biophysica Acta, 1016 (1990) 280–28
Elsevie

BBABIO 43184

Characteristic fluorescence components in photosynthetic pigment system of a marine dinoflagellate, *Protogonyaulax tamarensis*, and excitation energy flow among them. Studies by means of steady-state and time-resolved fluorescence spectroscopy

Mamoru Mimuro [1], Naoto Tamai [2,*], Takashi Ishimaru [3,**] and Iwao Yamazaki [2,*]

[1] *National Institute for Basic Biology,* [2] *Institute for Molecular Science, Okazaki, Aichi and* [3] *Ocean Research Institute, University of Tokyo, Nakano, Tokyo (Japan)*

(Received 5 September 1989)
(Revised manuscript received 1 December 1989)

Key words: Energy transfer; Fluorescence spectroscopy; Peridinin; Photosynthesis; Dinoflagellate; (*P. tamarensis*)

Excitation energy flow in intact cells of the marine dinoflagellate *Protogonyaulax tamarensis* was studied by steady-state and time-resolved fluorescence spectroscopy in the picosecond time range. At 15 °C, one dominant emission band was found at 684 nm (F684) with a minor band at 673 nm (F673), irrespective of the excitation conditions of Chl *a*, Chl *c* and peridinin. The 684 nm emission was DCMU-sensitive. At −196 °C, four major emission bands originating from Chl *a* were resolved at F670, F683, F689 and F698, as well as a minor component at F724. The F670 and F683 correspond, respectively, to the F673 and F684 at 15 °C. F689 was the strongest and assigned to a comparable component at F695, a characteristic band of CP-47. F698 and F724 were assigned to Photosystem (PS) I Chl *a*. When peridinin was excited, the F670 increased selectively, indicating that it is the energy acceptor of peridinin. Time-resolved fluorescence spectra at −196 °C revealed all the components above as well as a new component at F709. Upon the excitation of peridinin, the rise and decay kinetics of the component bands clearly showed the energy flow in the order of F670, F683 and F689, and also indicate that the energy is distributed to PS I antenna complexes via F683 (spill-over) but not through F689. Chl *c* does not mediate the energy flow from peridinin to Chl *a*. The transfer time from peridinin to the acceptor Chl *a* (F670) was estimated to be shorter than 20 ps at −196 °C. Based on these results, a model for the energy flow in *P. tamarensis* was proposed.

Introduction

Two kinds of compound function as antenna pigments in photosynthesis; one is porphyrin (chlorophyll) and the other, polyene (carotenoid). These two are distinct in their physical and chemical properties, and in their in vivo synthetic pathways. Both of them are always found in photosynthetic organisms; however, their in vivo constitution is different.

Carotenoid is known to function in algae [1] and in photosynthetic bacteria [2]. Especially in some phyla of algae, carotenoid is the main light-harvesting antenna pigment [1]. The quantum yield of carotenoid for photosynthesis is comparable to that of Chl *a* [3] and transfer efficiency to chlorophyll is known to be high [4]. However, the energy transfer process from carotenoid to chlorophyll is not well characterized, compared to that of chlorophyll and phycobiliproteins. An electron-exchange mechanism is proposed for the carotenoids-to-chlorophyll process [5], contrary to the Förster mechanism for chlorophyll and phycobiliproteins [6]. The electron exchange mechanism requires a close location of donor-acceptor pair (approx. 0.5 nm); thus, topology of the pigments in polypeptide(s) is a critical point.

Peridinin, an antenna pigment in dinoflagellates [1], is an allene carotenoid with a unique 4-iridenebutenoride structure [7]. Peridinin forms two kinds of pigment protein complex: water-soluble [8] and membrane-bound [9,10]. Both of them are functional in

* Present address: Department of Chemical Process Engineering, Faculty of Engineering, Hokkaido University, Sapporo, Japan.
** Department of Aquatic Biosciences, Faculty of Fisheries, Tokyo University of Fisheries, Minato, Tokyo, Japan.

Abbreviations: Chl, chlorophyll; DCMU, 3-(3,4-dichlorophenyl)-1,1-dimethylurea; F683, a representative expression of the emission band located at 683 nm; PCP, peridinin-chlorophyll protein; PS, Photosystem; RC, reaction center.

Correspondence: M. Mimuro, National Institute for Basic Biology, Myodaiji, Okazaki, Aichi 444, Japan.

photosynthesis. The water-soluble peridinin-chlorophyll protein (PCP) has been characterized in some detail, and it was shown that four peridinin molecules and one Chl *a* molecule are associated with a peptide of 35 kDa [11–13]. The energy-transfer mechanism in this complex, however, has not yet been elucidated. This is due mainly to lack of information on the time-dependent behavior of component(s) and fluorescence properties of carotenoids, which are critical for the analysis, as shown for the case of chlorophyll and phycobiliproteins [14,15].

In this study, we adopted two kinds of fluorescence spectroscopy for the analysis of energy flow in intact cells of the marine dinoflagellate *Protogonyaulax tamarensis*; steady-state and time-resolved spectroscopy in the picosecond time range. Our results show unique fluorescence components in this species, and a specific energy flow among them. The transfer time from peridinin to Chl *a* was estimated to be shorter than 20 ps at −196 °C.

Materials and Methods

Algal culture

A marine dinoflagellate, *P. tamarensis*, was cultured in an enriched seawater medium (modified T1 medium) [16] at 15 °C under a 12 h light (75 $\mu E/m^2$ per s) and 12 h dark regime. Cells in the stationary growth phase were harvested and used for measurements.

Steady-state spectroscopy

Absorption and fluorescence spectra were measured with a Hitachi 557 spectrophotometer and a Hitachi 850 spectrofluorometer, respectively. The spectral sensitivity of the fluorometer was numerically corrected with reference to the radiation profile of a substandard lamp with an known color temperature [14]. For measurements at −196 °C, 15% poly(ethylene glycol) 4000 was added to the medium to obtain homogeneous ice and samples were immersed in liquid nitrogen during the measurements.

All spectral data were transferred to a microcomputer (Hewlett-Packard model 216) and analyzed. The second derivative spectra were obtained by the method of Savitzky and Golay [17].

Time-resolved fluorescence spectroscopy

The time-resolved fluorescence spectra were measured with the apparatus reported previously [14,18–20]. Intensity of the excitation pulse (540 nm, 6 ps (fwhm)) was in a range of 10^8 to 10^9 photons/cm^2 per pulse, which was low enough to avoid singlet–singlet annihilation. The time-resolution of our optical set-up was 6 ps. The spectral sensitivity of the detection system (monochrometer and micro-channel plate photomultiplier (R2809U-01, Hamamatsu Photonics, Japan) [21]) was numerically corrected.

Deconvolution of the time-resolved spectra and estimation of lifetimes by convolution calculation with reference to the excitation pulse were carried out as reported previously [14,19,20].

Results

Steady-state fluorescence spectra at physiological temperature

The main photosynthetic pigments in *P. tamarensis* are Chl *a*, Chl *c* and peridinin. Peridinin accounts for more than 70% of total carotenoids [22,23]. The molar ratio of Chl *c* to Chl *a* is repoted to be 0.6 to 1.0 [22] and that of peridinin to Chl *a*, 1.2 to 2.0 [23], respectively.

Fig. 1A shows the fluorescence spectra of intact cells of *P. tamarensis* at 15 °C. The main emission is located at 684 nm (F684), with a small bump at 673 nm (F673) as evidenced by the second derivative spectrum (Fig. 1B). This emission pattern was almost the same, irrespective of the excitation conditions; 435 nm for Chl *a*, 465 nm for Chl *c* and 550 nm for peridinin. With excitation at 435 nm or 465 nm, a weak emission from Chl *c* was observed around 640 nm, whereas excitation at 550 nm did not result in any substantial fluorescence from Chl *c*. A relatively high intensity around 735 nm can be assigned to a mixed form of the vibrational structure of the two fluorescence components (F673 and F684).

On addition of DCMU ($5 \cdot 10^{-6}$ M), the 684 nm emission increased (Fig. 1C). The difference spectrum was essentially the same as the spectrum without DCMU, indicating that changes in the fluorescence yield are responsible for this increase. This phenomenon is known in higher plants as well as in algae which contain phycobiliproteins [24]. Since the 684 nm emission has been ascribed to CP-43 [25,26], the fluorescence properties of CP-43 in *P. tamarensis* might be very close to that of higher plants [26] or cyanobacteria [25]. A significantly high intensity of F673 suggests that part of the F673 is disconnected from the transfer sequence.

The excitation spectrum monitored at 735 nm differed from the absorption spectrum (Fig. 2); compared with the absorption spectrum, a contribution of the pigment(s) located in the wavelength region between 400 and 500 nm was clearly low. This suggests the presence of an uncoupled carotenoid in this wavelength region. The purified PCP is known to show absorption maxima at 470 and 510 nm [11–13]. A clear maximum around 535 nm suggests the presence of another type of pigment-protein complex combined with a red-shifted carotenoid. In the wavelength region for the Q_y band of Chl *a*, the excitation spectrum was similar to the

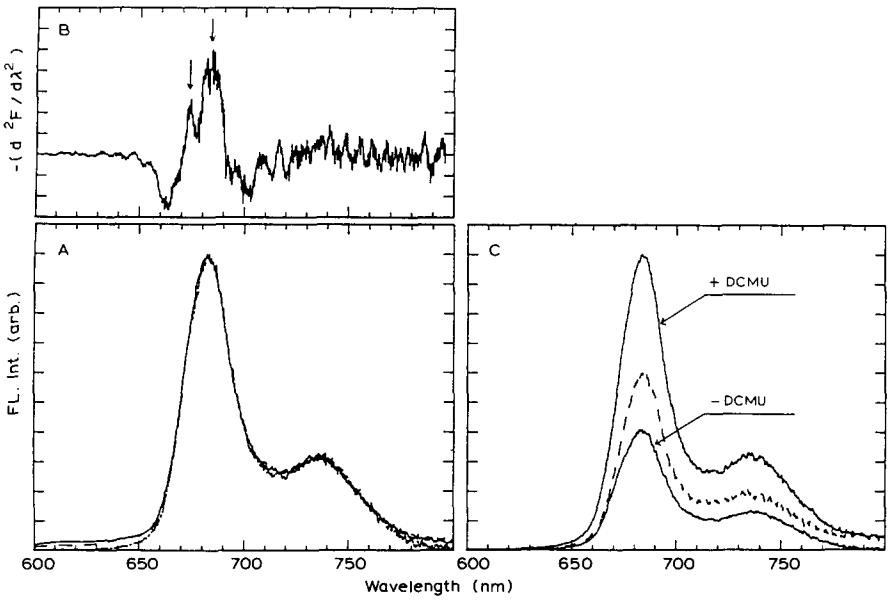

Fig. 1. Fluorescence spectra of *P. tamarensis* at 15 °C. In (A), the spectra were obtained by the excitation at 435 nm (———), 465 nm (- - - - -) and 550 nm (· – · – ·). The second-derivative spectrum was obtained on the spectrum excited at 550 nm and shown after inversion (B). In (C), DCMU-sensitive fluorescence (- - - -) was shown under the excitation at 550 nm, which was induced by the addition of $5 \cdot 10^{-6}$ M DCMU. For details, see the text.

absorption spectrum with a small difference in the narrower bandwidth, suggesting heterogeneity of the chlorophyll form in this species; the 670 nm absorbing form can be assigned as a major component in PS II antenna pigments.

Steady-state fluorescence spectra at −196 °C

The fluorescence spectrum at −196 °C is drastically different from that at 15 °C (Fig. 3). The main emission was located at 689 nm (F689) with a small but clear band at 670 nm (F670) (Fig. 3A), irrespective of the excitation conditions. The second-derivative spectrum (Fig. 3B) indicates the presence of two minor bands at 683 (F683) and 698 nm (F698). A small bump observed around 725 nm was not clearly resolved by the second-derivative spectrum. A distinct difference was observed in the emission intensity at F670 (Fig. 3C), because with excitation of peridinin (540 nm) the F670 was significantly higher than with excitation of Chl *a* (430 nm) or Chl *c* (460 nm). This clearly suggests that the F670 is an energy acceptor of peridinin. Emission from Chl *c* was dependent on the excitation conditions, showing variation in the emission maxima of 636, 638 and 643 nm by the excitations at 430, 460 and 540 nm, respectively. These results suggest the presence of multiple emission components and variable absorption fractions. The presence of two emission components of Chl *c* is also established in the pigment system of brown algae [27,28].

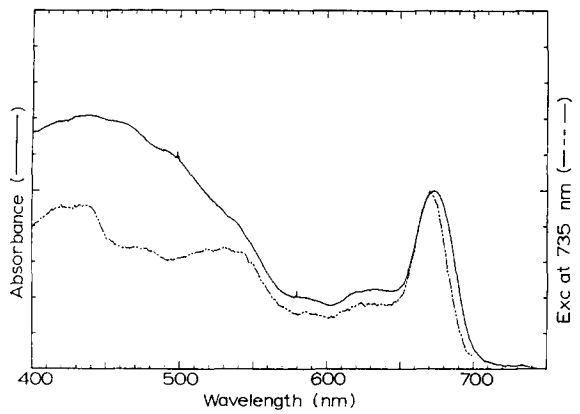

Fig. 2. Absorption (———) and excitation (· · — · · — · ·) spectra of *P. tamarensis* at 15 °C. Fluorescence was monitored at 735 nm. Two spectra were shown after normalization to the maximum of the Q_y band of Chl *a*.

In green plants and some algae, three typical fluorescence bands are commonly observed in the spectra at −196 °C [24]; F685, F695 and F735. Another band at F705 has been resolved by fluorescence polarization [29] and in spectra measured at 4 K [30]. It is known that F685 and F695 are attributed to PS II and the F735 to PS I [24]. A comparison of these assignment with the composition of *P. tamarensis* suggests some significant differences. Although the F685, F695 and F735 are appear to be absent in this species, we nevertheless assigned the F683 and F689 to the F685 and F695, respectively. We make this assumption for the following reasons. (a) F670 was observed under both temperature conditions (Figs. 1 and 3); (b) the F684 was DCMU-sensitive at 15 °C and was also observed at −196 °C (F683); and (c) the F689 was the most intense component and on that basis is similar to the F695 which is a major emission component. The temperature-dependent

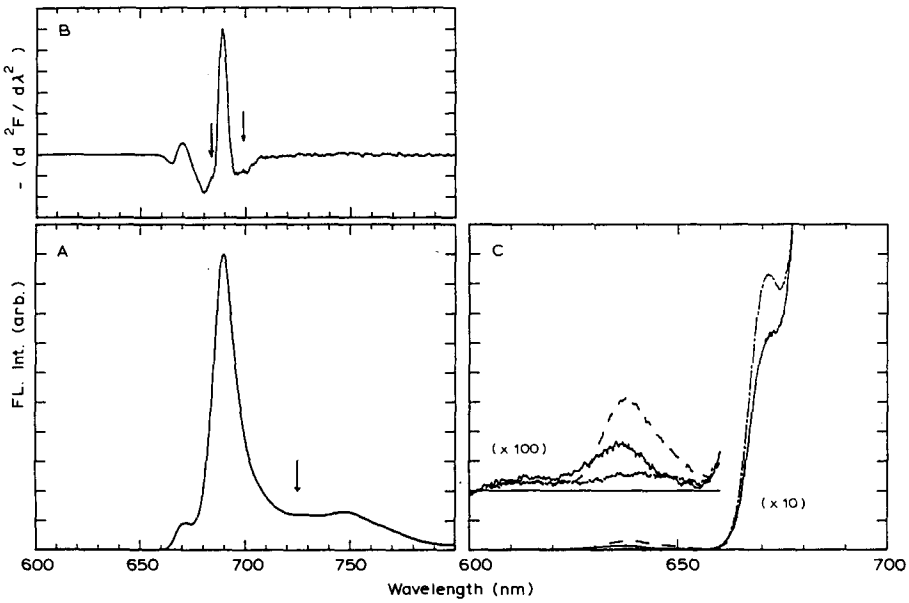

Fig. 3. Fluorescence spectra of *P. tamarensis* at −196 °C (A) under the excitation at 540 nm and its second-derivative spectrum (B). In (B), the spectrum is shown after inversion. (C) is the magnified spectra under the excitation of 430 nm (———), 460 nm (- - - - - -) and 540 nm (·—·—·). Arrows indicate the locations of component bands at 724 nm (A), and 683 and 698 nm (B).

behaviour of these components is essentially identical to that observed in spinach chloroplasts [24]. This assignment was confirmed by the time-resolved fluorescence spectra (see later).

At −196 °C, two absorption bands were observed in the Q_y band region of Chl *a*; around 670 and 683 nm (Fig. 4). There is probably the third at 695 nm which most probably corresponds to the F698, detected by the second-derivative spectrum (Fig. 3B, and confirmed by the time-resolved spectra (Fig. 5)). However, the component(s) located at wavelengths longer than 700 nm was substantially absent, contrary to organisms which have a strong fluorescence beyond 700 nm [31].

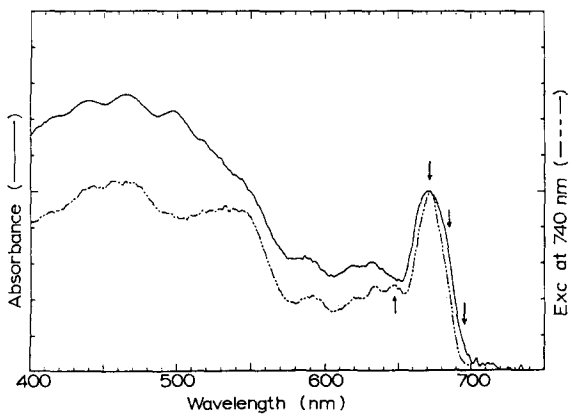

Fig. 4. Absorption (———) and excitation (·—·—·—·) spectra of *P. tamarensis* at −196 °C. Fluorescence was monitored at 740 nm. Arrows indicate the locations of the component bands. Two spectra were shown after normalization to the maximum of the Q_y band of Chl *a*, For details, see the text.

The excitation spectrum at −196 °C (Fig. 4) was essentially similar to the spectrum measured at 15 °C (Fig. 2) in that the lower contribution of the shorter

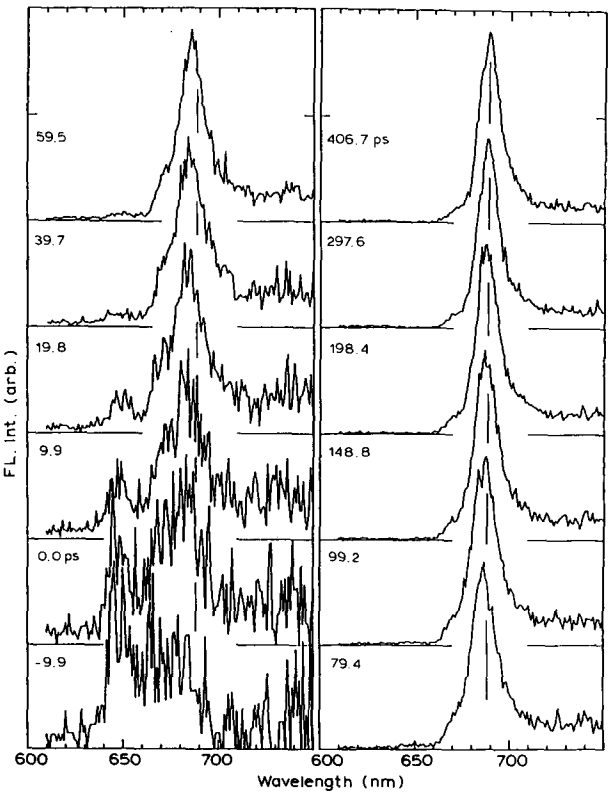

Fig. 5. Time-resolved fluorescence spectra of *P. taramensis* at −196 °C under the preferential excitation of peridinin (540 nm). Each spectrum was shown after normalization to the maximum intensity. Vertical line indicates the location of the fluorescence maximum 400 ps after the pulse. For details, see the text.

wavelength region and the high contribution of peridinin, Chl *c* and *a*, compared with the absorption spectrum. A narrower bandwidth of Chl *a* than that in the absorption spectrum indicates heterogeneity of the Chl *a* population. A characteristic band was observed at 647 nm, which presumably corresponds to the longer emission component from Chl *c* (Fig. 3C, and confirmed by the time-resolved spectra (Fig. 5)). Together with the 635-nm-absorbing form of Chl *c*, the 647 nm component can be assigned as a native constituent of the Chl *c* in this species.

Time-resolved fluorescence spectra

Time-resolved fluorescence spectra were measured at −196 °C to obtain better spectral resolution, and for the simultaneous detection of the PS I emission. Fig. 5 shows the normalized time-resolved fluorescence spectra under the preferential excitation of peridinin at 540 nm; however, Chl *a* and Chl *c* partly absorb the 540 nm light. Just after the excitation, a clear band was detected around 649 nm, originating from Chl *c*. This band corresponds to the 647 nm absorption band observed in the steady-state spectrum (Fig. 4). Other components located at 670 and 683 nm became evident with time. The decrease in the intensities of the 649 nm component was very fast (within 50 ps). The 683 nm maximum was observed 10 ps after the excitation pulse. However, location of the maximum gradually shifted from 683 nm and finally reached 689 nm at 300 ps after the pulse, as shown by a vertical line in the figure. Even in this time range, a significant intensity was observed around 670 nm, indicating the presence of a long-lived component. The spectra after 400 ps were invariant up to 1 ns (data not shown). In the wavelength region longer than 700 nm, there was no clear emission maximum, which is expected to arise from PS I component(s). However, one should notice a clear bump around 700 nm, especially in the spectra at 198.4 and 297.6 ps (Fig. 5). This suggests the presence of more than one band in this wavelength region.

Identification of component bands by deconvolution of the time-resolved fluorescence spectra

Since several fluorescence components were detected in the time-resolved spectra (Fig. 5), the spectra were resolved into components by deconvolution with the assumption of Gaussian band shape as a function of wavenumber. We assumed a minimum four components (F649, F670, F683 and F689) which were clearly observed in the time-resolved spectra. Additionally, F698 and F724 were also assumed, based on the second derivative spectrum (F698, Fig. 3B) or a clear bump in the fluorescence spectrum (F724, Fig. 3A). Deconvolution with these six components, however, did not give a better fit (data not shown); thus, an additional component located at 709 nm was introduced. Using three

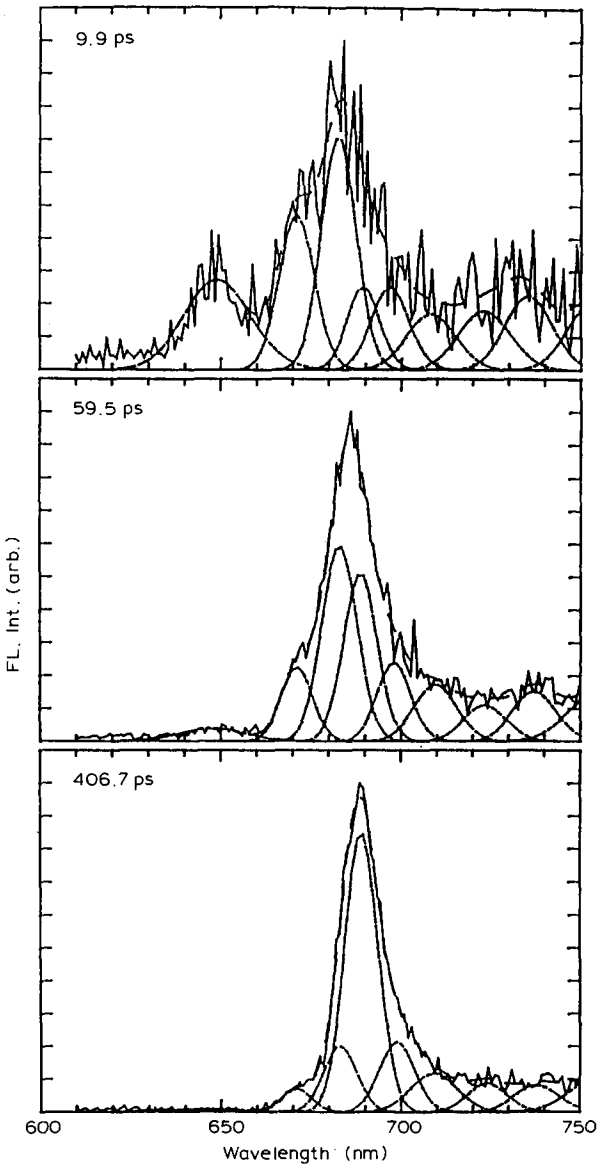

Fig. 6. Deconvolution patterns of the time-resolved fluorescence spectra. Deconvolution was carried out on the spectra shown in Fig. 5. Gaussian band shape was assumed as a function of wavenumber. (———), observed spectra; (·····), component band and (- - - - -), sum of component bands. For details, see the text.

parameters with variable intensities we obtained a better fit, and the typical changes in intensity of components with time are depicted in Fig. 6. Two additional bands were also necessary for the best fit (F737 and F755) which were assigned to the vibrational bands. In the initial time range, the intensities of F649 and F670 were high. Concomitant with the disappearance of these two, the maximum at 683 nm became evident, and finally the F689 was dominant.

Decay kinetics and energy transfer sequence

Rise and decay curves of individual components (Fig. 7) were estimated by the relative intensities of

components in the spectra at particular times and the actual number of photons observed for the respective spectra. As for F649, a reliable decay curve was obtainable only in the initial time range (up to 100 ps, see Fig. 5), because of a poor signal-to-noise ratio in the later time range. The decay curve of F670 was not exponential, indicating the presence of two decay components; a fast decaying and a very long-lived component. The latter component is probably responsible for a higher fluorescence intensity at 670 nm in the steady-state spectrum. The F683 and F689 show exponential decay. The kinetics of three PS I components (F698, F709 and F724) were similar to each other and their decay was faster than that of F689.

The sequence of energy transfer among the components was estimated by shift of the time when the maximum intensity was observed. A sequential shift was observed in the order of F670, F683 and F689; however, this was not the case between F689 and the components corresponding to PS I (F698, F709 and F724). This clearly indicates that the energy transfer to PS I components does not occur through F689; F683 is most probably an energy distributor to the PS I components, which is known as 'spill over' process.

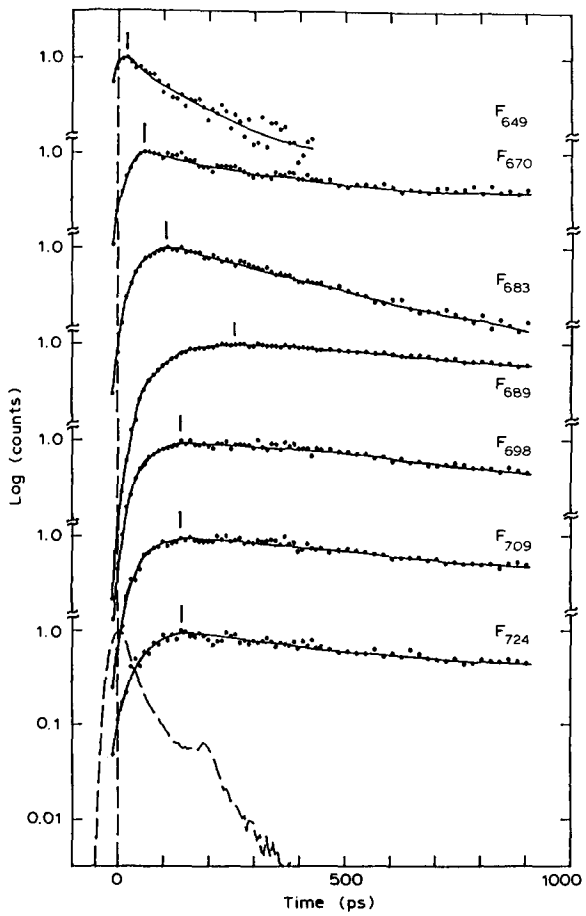

Fig. 7. Rise and decay curves of individual fluorescence components. Vertical line shows the time zero and broken lines, pulse profile. Small bars over the rise and decay curves indicate the time when the maximum intensity was observed.

TABLE I

Lifetimes of individual fluorescence components in P. tamarensis at −196 °C

Lifetimes were estimated by convolution calculation with the assumption of exponential decay. τ, lifetimes and A, amplitude.

	Rise term	Decay term			
	τ (ps)	τ_1 (ps)	A_1	τ_2 (ps)	A_2
F649		40	0.85	235	0.15
F670	18	55	0.79	1250	0.21
F683	55	75	0.85	350	0.15
F689	250	350	0.90	1250	0.10
F698	91	115	0.83	1110	0.17

Lifetimes of individual components were estimated by convolution calculation with the assumption of exponential decay kinetics (Table I). A rise term was not resolved in the kinetics of F649 and its decay was biphasic. There were two decay components with the lifetimes of 40 and 235 ps. On the other hand, a clear rise term was found in the F670 (18 ps), and its decay times were 55 and 1250 ps. Judging from the mismatch of decay constants between the decay of F649 and the rise of F670, Chl *c* (F649) is not the energy donor to F670. A fast decay of the F670 corresponds to the rise of the F683, indicating direct energy transfer from F670 to F683. The rise of F689 was slow (250 ps); it does not correspond to the decay of F683. Contrary to this, the rise of F698 was 91 ps, close to the decay of F683 (75 ps). When we assume that energy transfer occurs from F683 to both of F689 and F698 with an equal probability, the lifetime of F683 could be estimated to be 67 ps ($1/91 + 1/250 = 1/67$). This value is very close to our estimation (75 ps). This agreement supports the idea that F683 is the energy distributor to PS I component(s). The rise and decay constants of F709 and F724 were almost the same as those of F698 (data not shown), as suggested by essentially the same decay kinetics (Fig. 7). The lifetime of the main PS I component was about 110 ps with an amplitude of more than 80%. This is very short, compared with the lifetime of F735 in spinach chloroplasts at −196 °C (2.22 ns, Mimuro et al., unpublished data). This short lifetime is responsible for a weak fluorescence in the steady-state spectrum.

Discussion

Fluorescence components

Steady-state and time-resolved fluorescence spectra clearly revealed the presence of several fluorescence components of Chl *a* in *P. tamarensis* at −196 °C; F670, F683, F689, F698, F709 and F724. The former

three are assigned as PS II components, and the remaining three, PS I. The F689 is assigned as a comparable component to F695, a characteristic band of CP-47 [25,26]. This suggest that CP-47 in dinoflagellates could be different from that of higher plants, contrary to CP-43 whose fluorescence properties were suggested to be similar. Since CP-43 is ascribed to the energy donor to RC II, a structurally and energetically definite interaction might be necessary between the P-680 and the energy donor to it.

A remarkable feature was observed in the fluorescence components of PS I. The amount of absorption component at the wavelength longer than 700 nm were very small (Figs. 2 and 4). This is one of the reasons for a weak fluorescence of PS I. The other reason was a fast decay of fluorescence (110 ps for the main component). This is a unique feature of the pigment system of dinoflagellates; in higher plants or green algae, the lifetimes of the main PS I emission (F735 or F720) were estimated to be 3.1 ns [32] or 2.3 ns [33]. In *P. tamarensis*, a rise time of the PS I components is close to the decay of F683 (Table I). This is contradictory to the case of spinach chloroplasts, where the rise and decay between F685 and F735 is reported to be different [34–36]. However, comparison of the difference is not straightforward, because F698 is the direct energy acceptor of F683, on the contrary, F735 might be a final energy acceptor with an intermediate component(s) in the transfer sequence from F685.

The presence of F735 at low temperature is obscure in dinoflagellates [4] and also in diatom [37]. If this component arises from the peripheral antenna of PS I (LHCIb) [38], this polypeptide might be missing in this phylum. Or F735 might be replaced with F725 as similar to the case of green algae (F720) [24].

Chl *c* heterogeneity was also found. There were multiple emission components; 638 nm by the excitation at 460 nm (Fig. 3) and a significantly red-shifted emission (649 nm) by the 540 nm excitation (Figs. 3 and 5). The red-shifted component might originate from the 647 nm absorption band (Fig. 4). The presence of two types of Chl *c* was also shown in the antenna complex isolated from a brown alga *Dictyota dichotoma* [27,28]. This phenomenon might be general feature of the pigment system consisting of Chl *a*, Chl *c* and carotenoids.

Decay kinetics and energy transfer

As shown in Fig. 7, the decay kinetics of the fluorescence components were essentially exponential, except for F670. This is different from the case of phycobiliproteins, in which the decay kinetics proportional to the square root of time is applicable [39]. This difference might originate from difference in the structure of pigment system.

Energy flow among the components was clearly suggested by the rise and decay kinetics (Fig. 8). When

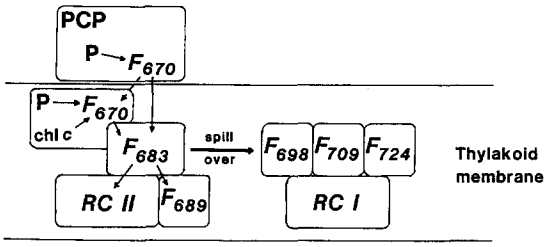

Fig. 8. Schematic model of energy flow in the pigment system of *P. tamarensis*. Except for PCP, individual components represent spectral forms, not the associating polypeptides. The broken line indicates the possible energy flow, but it is as yet undefined. P, peridinin and RC, reaction center. The direct energy donor to RC I is unclear. For details, see the Discussion.

peridinin was excited, the energy was transferred to F670, then to F683 and finally to F689. Chl *c* is not involved in the transfer sequence from peridinin to Chl *a*. The direct energy transfer from carotenoid to Chl *a* was also observed in fucoxanthin-Chl *a/c* protein assemblies isolated from brown algae, and Chl *c* does not mediate the energy transfer from fucoxanthin to Chl *a* [27,28]. The decay of F683 can be explained by the energy transfer to F689 and F698 (Table I) with the assumption of an equal probability, and thus it is a basis for that the F683 is the energy distributor in the pigment system of *P. tamarensis*. The kinetics of three PS I components were almost the same, suggesting a fast transfer among these three components.

The above mentioned transfer scheme is obtained basically by the analysis at −196 °C, where all the reaction center (RC) are closed. In principle, this scheme is applicable to the case at physiological temperature with open RCs. Changes in the absolute values for the transfer times are to be expected, because a larger fraction of energy sensitized by peridinin is tansferred to open RC II. The transfer to PS I component (spill-over), therefore, might be largely affected under the physiological condition.

The transfer time from peridinin to Chl *a* could not be measured by the decay of peridinin fluorescence, thus it was estimated by the rise of the acceptor Chl *a* (F670). So far fluorescence was not detected in the wavelength region from 550 to 620 nm, even with the time-resolution of 6 ps (data not shown). This observation confirms that the estimated fluorescence yield of carotenoid is lower than 10^{-5} [40]. The transfer time, estimated from the rise term of the F670 was 18 ps at −196 °C. At this experimental stage, the temperature dependency of transfer time from carotenoid to chlorophyll is not clearly elucidated. Due to a smaller resonance condition between donor and acceptor at low temperature, a slower transfer can be expected, regardless of the transfer mechanism [5,6]. In the case of photosynthetic bacteria, the transfer time at −196 °C is reported to be more than twice of that at room tempera-

ture [41]. If this is applicable to the case for energy transfer from carotenoid to chlorophyll, the transfer time from peridinin to Chl *a* is estimated to be shorter than 9 ps at physiological temperature. This value is in the range of 3 ps for bacterial antenna [42,43] and the synthetic compounds (10 ps [44]), and agrees with the observed singlet lifetime of carotenoid [40].

Acknowledgements

The authors express their thanks to the Instrument Center, Institute for Molecular Science, for the operation of picosecond spectroscopy, and to Drs. Y. Fujita and S. Itoh for their stimulative discussion during this study. They thank Professor E. Gantt, University of Maryland, for her critical reading of the manuscript, and Mr. Y. Nasu, National Institute for Basic Biology, for the aid of preparation of manuscript. This work was supported in part by the Grant-in-Aid, for the Scientific Research from the Ministry of Education, Science and Culture, Japan to MM (01300009, 01302064).

References

1 Siefermann-Harms, D. (1985) Biochim. Biophys. Acta 811, 325–355.
2 Van Grondelle, R. and Sundström, V. (1988) in Photosynthetic Light-Harvesting Systems: Organization and Function (Scheer, H. and Schneider, W., eds.), pp. 403–438, Walter de Gruyter, Berlin.
3 Tanada, T. (1951) Am. J. Bot. 38, 276–283.
4 Govindjee, Wong, D., Prezelin, B.B. and Sweeney, B.M. (1979) Photochem. Photobiol. 30, 405–411.
5 Dexter, D.L. (1953) J. Chem. Phys. 21, 836–850.
6 Förster, T. (1948) Ann. Phys. Leipzig. 2, 55–75.
7 Johansen, J.E., Svec, W.A., Liaaen-Jensen, S. and Haxo, F.T. (1974) Phytochemistry 13, 2261–2271.
8 Haidak, D.J., Mathews, C.K. and Sweeney, B.M. (1966) Science 152, 212–213.
9 Boczar, B.A., Prezelin, B.B., Markwell, J.P. and Thornber, J.P. (1980) FEBS Lett. 120, 243–247.
10 Boczar, B.A. and Prezelin, B.B. (1987) Plant Physiol. 83, 805–812.
11 Song, P.S., Koka, P., Prezelin, B.B. and Haxo, F.T. (1976) Biochemistry 15, 4422–4427.
12 Koka, P. and Song, P.S. (1977) Biochim. Biophys. Acta 495, 220–231.
13 Haxo, F.T., Kycia, J.H., Sommers, G.F., Bennet, A. and Siegelman, H.W. (1976) Plant Physiol. 57, 297–303.
14 Mimuro, M., Yamazaki, I., Tamai, N. and Katoh, T. (1989) Biochim. Biophys. Acta 973, 153–162.
15 Holzwarth, A.R. (1987) In The Light Reaction (Barber, J., ed.), pp. 95–157, Elsevier, Amsterdam.
16 Ogata, T., Ishimaru, T. and Kodama, M. (1987) Marine Biol. 95, 217–220.
17 Savitzky, A. and Golay, M.J.E. (1964) Anal. Chem. 36, 1627–1639.
18 Mimuro, M., Yamazaki, I., Tamai, N., Itoh, S. and Satoh, K. (1988) Biochim. Biophys. Acta 933, 478–486.
19 Shimada, K., Mimuro, M., Tamai, N. and Yamazaki, I. (1989) Biochim. Biophys. Acta 935, 72–79.
20 Mimuro, M., Nozawa, T., Tamai, N., Shimada, K., Yamazaki, I., Lin, S., Knox, R.S., Wittmershaus, B.R., Brune, D.C. and Blankenship, R.E. (1989) J. Phys. Chem. 93, 7503–7509.
21 Yamazaki, I., Tamai, N., Kume, H., Tsuchiya, H. and Oba, K. (1985) Rev. Sci. Instrum. 56, 1187–1194.
22 Prezelin, B.B. (1976) Planta 130, 225–233.
23 Prezelin, B.B. and Alberte, R.S. (1978) Proc. Natl. Acad. Sci. USA 75, 1801–1804.
24 Murata, N. and Satoh, K. (1986) in Light Emission by Plants and Bacteria (Govindjee, Amesz, J. and Fork, D.C., eds.), pp. 137–159, Academic Press, New York.
25 Yamagishi, A. and Katoh, S. (1983) Arch. Biochem. Biophys. 225, 836–846.
26 Tang, X.-S. and Satoh, K. (1984) Plant Cell Physiol. 25, 935–945.
27 Katoh, T., Mimuro, M. and Takaichi, S. (1989) Biochim. Biophys. Acta 976, 233–249.
28 Mimuro, M., Katoh, T. and Kawai, T. (1990) Biochim. Biophys. Acta 1015, 450–456.
29 Garab, G.I. and Breton, J. (1976) Biochem. Biophys. Res. Commun. 71, 1095–1102.
30 Kramer, H.J.M. and Amesz, J. (1982) Biochim. Biophys. Acta 682, 201–207.
31 Butler, W.L., Tredwell, C.J., Malkin, R. and Barber, J. (1979) Biochim. Biophys. Acta 545, 309–315.
32 Butler, W.L. and Norris, K.H. (1963) Biochim. Biophys. Acta 66, 72–77.
33 Mar, T., Govindjee, Singhal, G.S. and Merkelo, H. (1972) Biophys. J. 12, 797–808.
34 Reisberg, P., Nairn, J.A. and Sauer, K. (1982) Photochem. Photobiol. 36, 657–661.
35 Pellegrino, F., Dagen, A., Sekuler, P. and Alfano, R.R. (1983) Photobiochem. Photobiophys. 6, 15–23.
36 Wittmershaus, B.R., Nordlund, T.T., Knox, W.H., Knox, R.S., Geacintov, N.E. and Breton, J. (1985) Biochim. Biophys. Acta 806, 93–106.
37 Caron, L., Jupin, H. and Berkaloff, C. (1983) Photosynth. Res. 4, 21–33.
38 Lam, E., Ortiz, W. and Malkin, R. (1984) FEBS Lett. 166, 10–14.
39 Yamazaki, I., Mimuro, M., Murao, T., Yamazaki, T., Yoshihara, K. and Fujita, Y. (1984) Photochem. Photobiol. 39, 233–240.
40 Wasielewski, M.R. and Kispert, L.D. (1986) Chem. Phys. Lett. 128, 238–243.
41 Van Grondelle, R., Bergström, H., Sundström, V. and Gillbro, T. (1987) Biochim. Biophys. Acta 894, 313–326.
42 Wasielewski, M.R., Tiede, D.M. and Frank, H.A. (1986) in Ultrafast Phenomena, V (Springer Series in Chemical Physics, Vol. 46), (Fleming, G.R. and Siegmann, A.E., eds.), pp. 388–392, Springer, Berlin.
43 Sundström, V., Bergström, H., Gillbro, T., Van Grondelle, R., Westerhuis, W.H.J., Niederman, R.A. and Cogdell, R.J. (1988) in Photosynthetic Light-Harvesting Systems; Organization and Function (Scheer, H. and Schneider, W., eds.), pp. 513–518, Walter de Gruyter, Berlin.
44 Wasielewski, M.R., Liddell, P.A., Barrett, D., Moore, T.A. and Gust, D. (1986) Nature 322, 570–572.